Towards characterization of intrinsic and stratigraphic Q in VSP data with information measures

Siming Lv and Kris Innanen

ABSTRACT

The problem of distinguishing between intrinsic Q and stratigraphic filtering is a classical example of non-uniqueness in seismic data analysis. Two very different mechanisms affecting propagating waves – reverberations between thin layers and transformation of mechanical energy to heat – produce almost identical effects. A version of the Shannon entropy, defined on snapshots of a VSP wave field, has been proposed to discuss these two influences, but it so far has been used to argue that the distinction is not as meaningful as we might think. In this project the entropy calculation is extended in time domain and also to frequency domain, aiming to locate what can be separated between these two effects. Conditional probabilities in which correlation of wave field values with neighbouring values is incorporated, rather than a statistical PDF histograms of single instances of particular wave field values. 1D VSP modelling codes and a range of well logs are used to investigate the separability of intrinsic/extrinsic sources of attenuation and dispersion. Progress of this kind will have significant impact on reservoir characterization where viscosity changes are expected: such changes can be tied to intrinsic Q but not extrinsic Q. The results, in which the various processes produce noticeable differences in entropy, indicate that this is a promising line of inquiry. Parameters like bin size have a large effect on the entropy, especially at late times, so that the footprint of bin size is studied in detail.

INTRODUCTION

Stratigraphic filtering is the special term used to describe apparent amplitude dissipation caused by reflections, especially internal multiples, in contrast with dissipation caused by the absorption factor Q (Aki and Richards, 1980). It happens when an incident wave traverses an absorption-free, finely layered sequence and excites a complex series of reflecting events.

Geophysicists' attention on this phenomenon was first drawn by the fact that reflection travel time discrepancies exist between seismic and well log data; amplitudes are frequency-dependent attenuated and dispersed in sedimentary layers, etc. (more specific statement can be found in paper of Resnick, 1990). Both absorption and stratigraphic filtering contribute to these effects. It has been since verified by many experiments and observations that the scattered multiples have attenuating effects on the transmitted wave which highly resemble those caused by absorption: decaying and spreading waveform, reducing the high-frequency content of the initial disturbance and appends incoherent coda to the signal (Figure 1). Since its mechanisms have origins not based on intrinsic rock properties, it can be regarded as an extrinsic Q factor in contrast with intrinsic Q.

Ever since O'Doherty and Anstey (1971) pointed out the equivalent importance between stratigraphic attenuation and absorptive attenuation in periodic layering section, significant effort has been expended in developing methods which attempt to distinguish between intrinsic and extrinsic Q (Hauge, 1981; Spencer, 1977, 1982; Stewart, 1984; Walden and Hosken, 1985). In a recent work, Margrave (2015) estimated intrinsic Q variation in a northern Alberta site by spectral ratio and dominant frequency methods and tried to isolate the stratigraphic effect by subtracting intrinsic Q from the total attenuation. Although the results did not fully meet expectations due to the barely satisfactory data quality and fail of including converted wave, it still proved the feasibility of separating stratigraphic attenuation and absorptive attenuation.

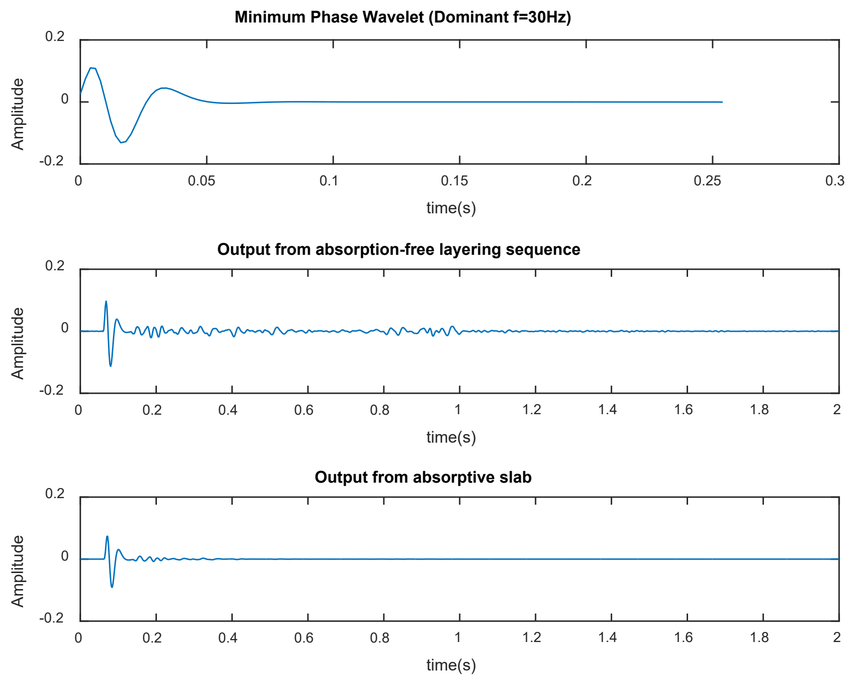

FIG. 1. The highly resembled amplitude attenuation effects of stratigraphic filtering and absorption

One important reason why geophysicists would like to distinguish intrinsic and extrinsic Q is that one of them is connected to important rock properties, and the other one is connected more closely with structural changes in rock properties. In unconventional heavy oil reservoirs, the viscosity of the fluid is a very important property. Since many heavy oil recovery methods such as the Steam-Assisted Gravity Drainage (SAGD) method are using a same exploiting strategy: reducing oil viscosity to let it flow spontaneously, a clear understanding of the viscosity of the reservoir is crucial to help designing production schemes, enhancing recovery and so on. While the viscosity in the borehole is relatively easy to be measured, it requires of extra strategy in the region between wells. Vasheghani and Lines (2009) analyzed the relationship between the heavy oil viscosity and intrinsic Q, showing that the viscosity of a cross-well section can be derived from the intrinsic Q measurement by Biot-Squirt theory (Lines, Vasheghani and Bording, 2013). Therefore, estimation of intrinsic Q free from effects of extrinsic Q is valuable for quantitative interpretation.

Innanen (2012) made the case that the disorder of the mechanical disturbances involved in a seismic wave was a common feature of both intrinsic and extrinsic Q. Treating each snapshot of a VSP wave field as a “sentence” written in an “alphabet” of allowable discrete values of the displacement, the Shannon entropy or information content of each snapshot could be calculated. The argument was that this allowed a single measure of the wave field to transition smoothly from characterization of multiples, to multiples below the resolution of the data, and to intrinsic Q.

The goal of this research is to use some of the same entropy ideas to consider intrinsic and extrinsic Q, but to extend and use them to help distinguish between the two attenuation mechanisms. This paper is organized as follows. In four different 1D zero-offset vertical seismic profile (VSP) models generated from an identical well log but with diverse attenuating conditions, first compute the original amplitude entropy (Innanen, 2013) with travel time advancement to monitor the information variation in wave field. Then modify some parameters to trace their footprint in the experiment. Utilize natural bound of seismic waveform afterwards to further develop a conditional entropy algorithm, test the reactions of intrinsic and extrinsic Q under the new algorithm. Finally, the process is repeated on well log data from three different work areas to ensure the result does not confine to a single area.

METHODOLOGY

Shannon Entropy

A promising way to investigate the thin bed reverberations which are the source of extrinsic Q, is to measure the amount of information in wave field. From this point of view, a wave field containing complex reflecting events can be thought as carrying considerable information in it whereas the wave field without a complex train of interbed multiples might be said to contain relatively small amount of information. In information theory, this is turned into a quantitative idea through the entropy.

We use Shannon entropy, which represents the exact value of the information in a message, to characterize the distributions of amplitudes in seismic wave fields. Shannon Entropy deals with uncertainty of the message. For a discrete random variable X with possible values $\{x_1, x_2, \ldots, x_n\}$ and their corresponding probability distribution $\{P(x_1), P(x_2), \ldots, P(x_n)\}$, Shannon defined entropy H about variable X as:

$$H(X) = \sum_{i=1}^{n} P(x_i) I(x_i) = -\sum_{i=1}^{n} P(x_i) \log_b P(x_i) \quad (1)$$

We generally take the base b=2, with corresponding unit of entropy H being "bit".

Among many characteristics of Shannon Entropy, there is one called additivity. For independent events X, Y who has entropy $H(X)$ and $H(Y)$. The entropy of sum of the events is just:

$$H(XY) = H(X) + H(Y). \quad (2)$$

In this research, we define the initial entropy (it is called initial entropy because another conditional entropy algorithm will be introduced in the later section) on snapshots of a seismic wave field, that is, distributions of displacement values in space at a fixed instant of time. According to Innanen (2012), if each snapshot consists of N data points (i.e. responses from N receivers), and every datum takes a displacement value u_i from m possible values, by enumerating the number of occurrences of a certain value u_i in the snapshot as $W(u_i)$, we can define probability of its occurrence as:

$$P(u_i) = \frac{W(u_i)}{\sum_{i=1}^{m} W(u_i)} \tag{3}$$

Then, Shannon entropy is calculated as in equation (1):

$$\mathrm{H} = -\sum_{i=1}^{m} P(u_i) \log_2 P(u_i) \tag{4}$$

Is possible to see from this entropy definition, the more possible values the displacement can have and the wider its probability distribution function (PDF) is, the bigger the Shannon entropy will be. Thus, H should be expected to go up when the disorder of the wave field increases. The rate at which this occurs may be a useful and sensitive measure of processes like absorption and stratigraphic filtering: if we can understand how each one affects the wave differently, it might even allow us to separate them.

Model Construction

As time increases, and the seismic wave propagates through a set of layers and reverberates, H should increase. Similarly, if the wave undergoes dispersion, this will also contribute to a growing entropy value. To confirm this, we designed some controlled trials using 1D zero-offset VSP data sets.

It is convenient for the analysis of a wave field across a range of spatial positions at given instants of time in a VSP data set. What is needed in order to systematically study the influence of extrinsic and intrinsic Q on such a wave is, then, a VSP modelling tool in which absorption and multiples can be turned on or off at will.

This is provided in tools written to support Margrave's research in 2014(a) about stratigraphic filtering and Q estimation. These tools make use of CREWES' MATLAB toolbox, in which we can design an artificial intrinsic Q distribution from P-wave velocity and density, given well logs according to an empirical relationship:

$$Q_v(z) = Q_0 \frac{v(z)-v_1}{v_0-v_1} + Q_1 \frac{v(z)-v_0}{v_1-v_0} \tag{5}$$

$$Q_\rho(z) = Q_0 \frac{\rho(z)-\rho_1}{\rho_0-\rho_1} + Q_1 \frac{\rho(z)-\rho_0}{\rho_1-\rho_0}. \tag{6}$$

These equations match Q_0 with v_0 and ρ_0, Q_1 with v_1 and ρ_1 then derive Q thorough out the objective depths from these two points. The values v_0, ρ_0, $v_1$and$\rho_1$are all available from standard well logs.

The final Q model is derived according to the following equation to combine the estimation.

$$\frac{1}{Q(z)} = \frac{1}{2}\left(\frac{1}{Q_v(z)} + \frac{1}{Q_\rho(z)}\right). \tag{7}$$

Once a defensible Q model has been determined, a VSP data set can be built by a propagator matrix method (Margrave and Daley, 2014b). In this approach, it is possible to turn on and off internal multiples, surface multiples, transmission loss and absorption in the finalized VSP data set. This way, the influence of these processes on the entropy, alone or together, can be studied.

Research Strategy

The initial study will use the same measure of entropy which is proposed by Innanen (2012) on some example well logs. In this algorithm the probabilities are directly determined from statistics, and therefore the information estimates do not contain any sensitivity to correlations between nearby wave field values. This is referred to as "zero order" source in the context of information theory for each data point is viewed as independently derived. After this initial study, new, more complex PDFs based on conditional probabilities are built up, allowing new information regarding correlations of adjacent data points to be included.

The calculation of the Shannon entropy of wave field snapshots requires us to define a range of possible amplitude values and then the probability distribution function can be derived from the statistics of wave field.

Some points worth paying attention to in this process are:

(1) The Shannon Entropy we are using deals with discrete distributions. This means we will have to define and use amplitude bins. Considering the dynamic range of VSP data, calculation costs as well as the measurement error of Matlab, the proper choice of amplitude binning is crucial, so that different kinds of information (primaries, multiples, etc., and their phase and amplitude behaviour) can be distinguished;

(2) Knowing that the wave field is the convolution of the source wavelet and the expression of subsurface structures on the wave, we expect that the source waveform has an important impact on the PDFs, an impact which does not vary with time. We proceed assuming that evaluation of wavelet amplitudes allows us to determine a proper wave field amplitude range and bin size.

Well logs and Data Analysis

Well logs

Well log data has been collected from a range of areas to be used in the analysis, to minimize the possibility that the results are special to one area:

(a) Two well logs from Blackfoot Oilfield in Alberta, Canada. Located 15km south-east of Strathmore (Figure 2): 1227 and 1409;

(b) Three well logs from work area near Hussar, Alberta, Canada (Figure 3): 12-27-025-21, 14-27-025-21 and 14-35-025-21;

(c) Two well logs separately from Gove and Comanche work area in Kansas, United States: Roemer-Bell #1-1(Figure 4) and Kissel 'A' No. 1-8(Figure 5).

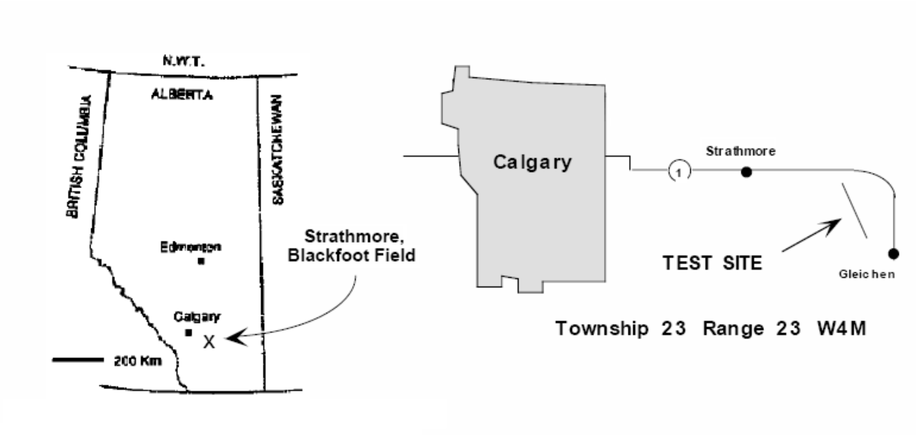

FIG. 2. Location of the Blackfoot Oilfield

FIG. 3. Location of Hussar wells

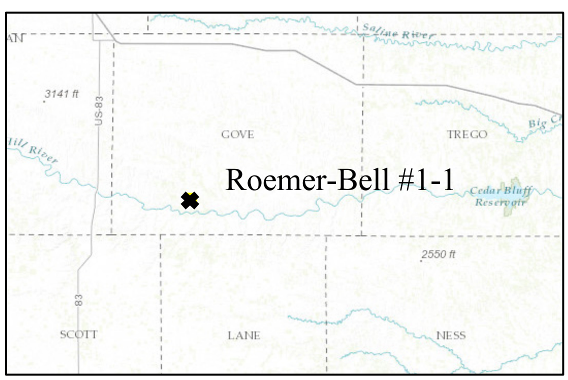

FIG. 4. Location of Kansas well Roemer-Bell #1-1

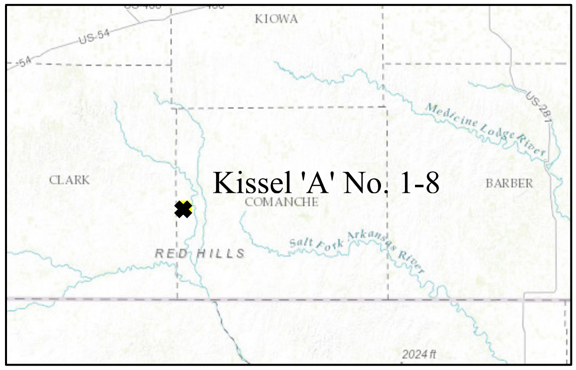

FIG. 5. Location of Kansas well Kissel 'A' No. 1-8

Data Analysis

A controlled series of Shannon entropy calculations was carried out on four different 1D VSP wave fields generated from the well logs: a) with only primaries; b) with primaries and internal multiples, c) with primaries and absorption and d) with primaries, internal multiples and absorption.

In experiment, we found that entropy reaction (trend and relative relationship) of all the tested wells were similar, indicating that the entropy calculation is robust. So, zooming in on the result of a particular well--Blackfoot 1227, allows the basic approach to be illustrated. Table 1 contains some key parameters that are used in the initial experiment. A "fake Q" model (Margrave, 2013) is created for 1227 and is plotted in Figure 6. The four VSP data sets are then calculated and presented in Figure 7. Using the amplitude binning strategy and equation (3), PDFs representing the probability of picking a particular wave value (i.e., particle displacement) at random from a snapshot of the VSP wave field are derived and shown in Figure 8. Then, with the equation (4) strategy, the entropy H of any desired time point in the wave field can be calculated. As we assume the wave field is "zero order", the total entropy value of the snapshot can be obtained by multiplying H by N times, making use of additivity in equation (2). Finally, the entropy variation with traveltime advancement of all wave fields is shown in Figure 9.

Table 1. Key parameters

Q		**Geophone**				**Amplitude Bin Size**
Minimum Q	Maximum Q	Interval(m)	Depth Range(m)	Dominant F of wavelet(Hz)	Maximum traveltime(s)	
20	220	0.5	0-1300	30	2.0	0.001

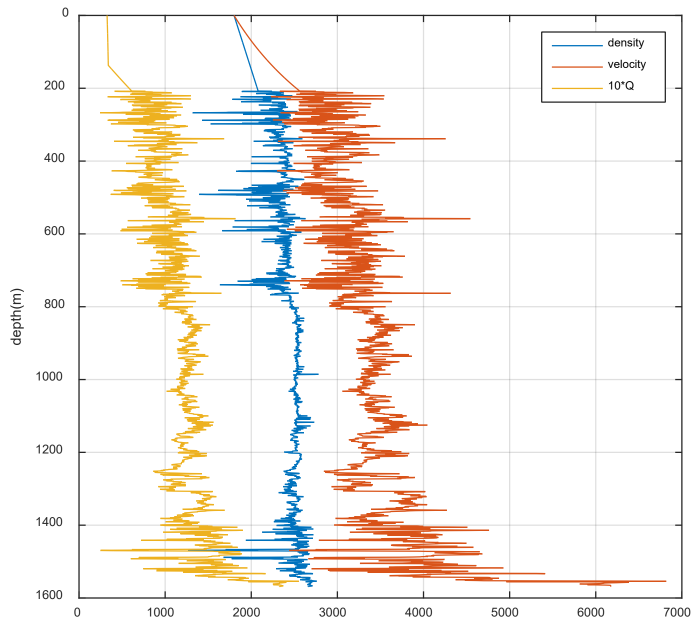

FIG. 6. Empirical estimated Q model from sonic (P velocity) and density logs of well “Blackfoot 1227”

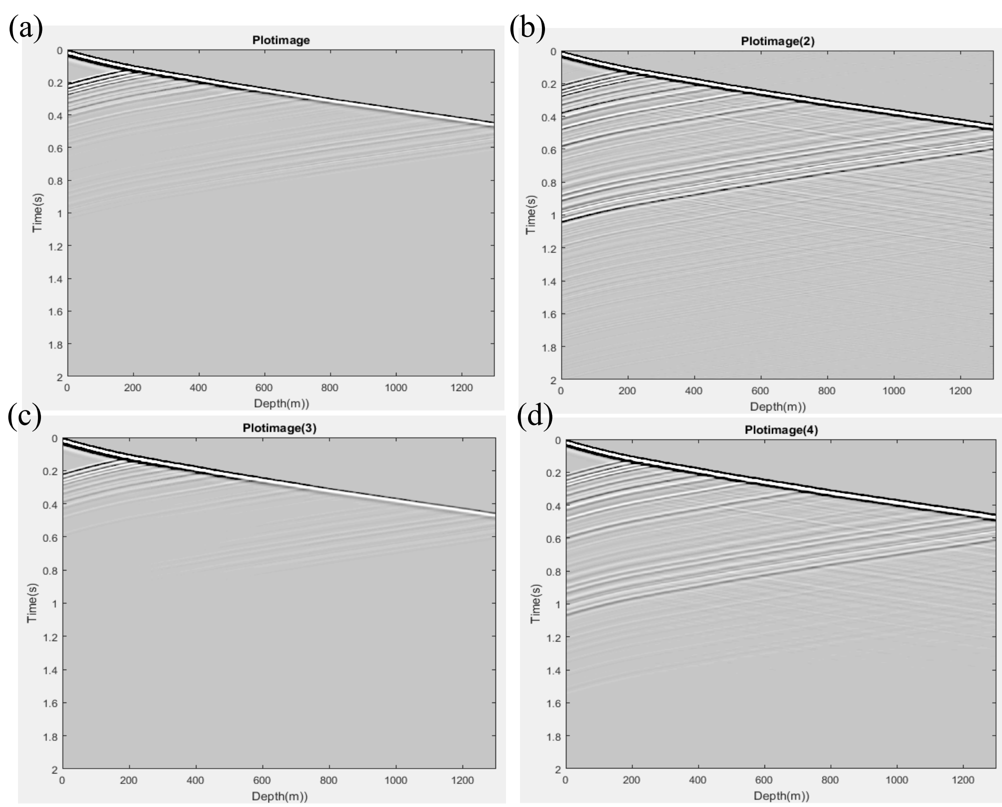

FIG. 7. VSP data sets, (a) primaries with no absorption or internal multiples (b) primaries with only internal multiples (c) primaries with only absorption (d) primaries with both absorption and internal multiples for well “Blackfoot 1227”. Transmission loss exists in all data sets.

In Figure 8 the estimated PDFs are plotted. Each row represents the PDF computed at a certain time, so scanning up and down vertically permits us to discuss the time variation of the probabilities of wave amplitude values. The most noticeable fact is, after a certain time, the PDFs become completely localized. This represents a baseline, or zero state, after all signal information has passed; noise and artifacts fill one bin of the histograms here. For example, in Figure 8a, the amplitude distribution is confined to times between 0.2-0.8s. By checking Figure 7a, we find it is caused by collection of strong waves in this time region.

Comparisons among 8a, 8b, 8c and 8d allow us to draw some preliminary conclusions:

(1) Existence of internal multiples extend the breadth of the PDFs to later arrival times and wider amplitude range, which, increase the disorder of wave field overall;

(2) Absorption impacts amplitude dispersion in exactly the opposite way: it shrinks the amplitude variation to a smaller range and consequentially reduces the disperse effect to earlier arrival times;

(3) With internal multiple and Q functioning at the same time. Amplitude dispersion is in a status between 8b and 8c where internal multiples and absorption are acting individually: it reaches later traveltime than 8c while the variation range shrinks to a slightly smaller value than 8b.

Outcome (3) appears to depend on the relative strength of internal multiples and absorption. But (1) and (2) suggest that the information measure H may be sensitive enough to distinguish between the two attenuation mechanisms.

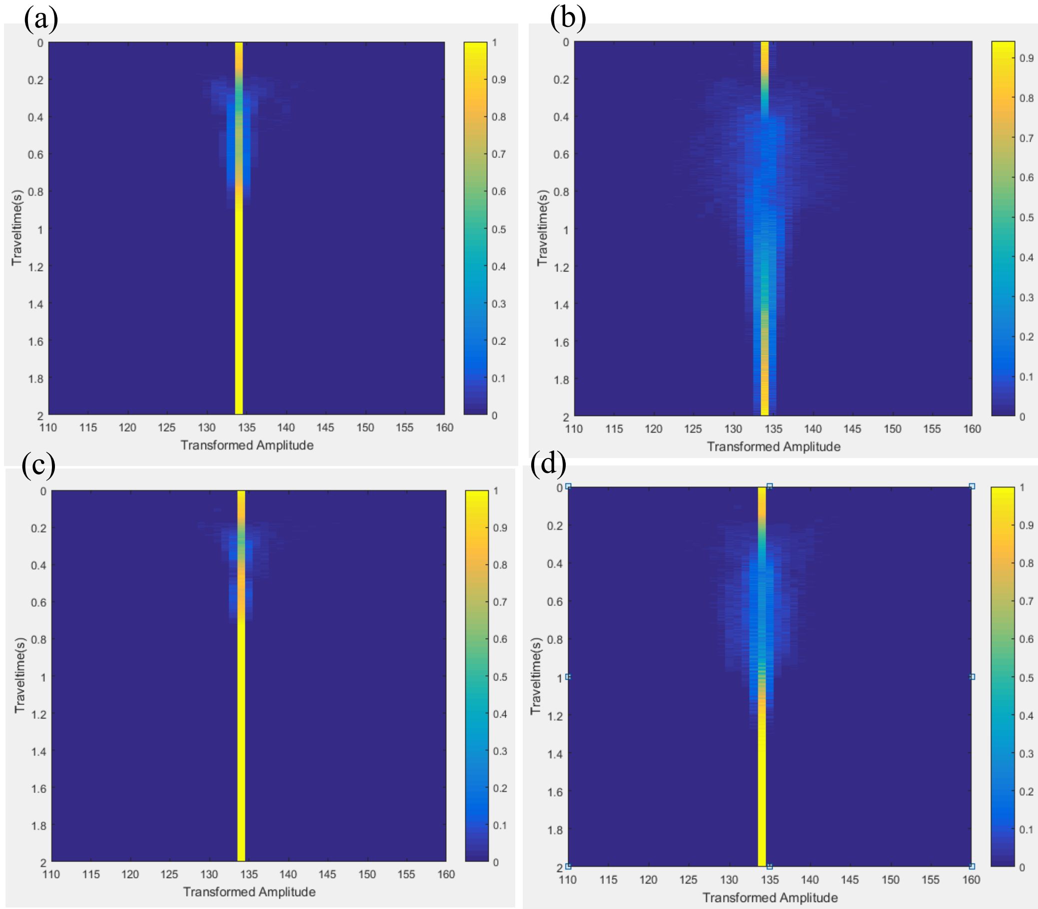

FIG. 8. Statistical PDF from VSP data sets (a) primaries with no absorption or internal multiples (b) primaries with only internal multiples (c) primaries with only absorption (d) primaries with both absorption and internal multiples built from Blackfoot 1227

In Figure 9, for all systems, entropy rises with increasing time in reaction to the amplitude dispersion that gradually took place in wave field. However, while the general trend of H curves reflects similar information increasement, investigating the difference among peaks of the H curves will provide us with clues to distinguish intrinsic and extrinsic Q.

Without stratigraphic filtering in system, the yellow and blue curves have low peak entropies at between 0.2s and 0.3s, which can be regarded as a direct response to the primaries generated from an "interface intensive region": 200m-400m. And comparing yellow curve to the blue one, the absorption in system contributes to an even smaller peak value.

After internal multiples being added to the system, the entropy curves (purple and red in Figure 9) reach higher peak entropies at latter time around 0.4s in contrast to the other two curves. From the delayed peak time we can infer that the first order multiples from the interface intensive region are making biggest efforts to the rise of entropy.

Presumably, the effect of absorption counteracts some scattering effects of the internal multiples by attenuating the amplitude, which explains why purple curve stays between red and blue ones. Considering this, it might be more precisely to say that, inside the wave field, internal multiples are scattering the amplitudes while absorption is attenuating amplitudes.

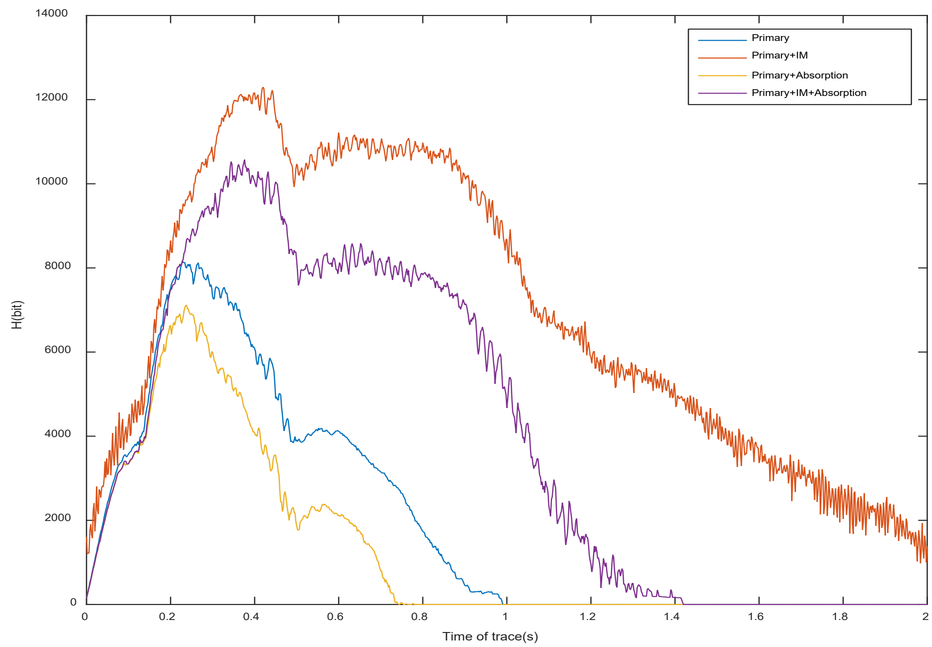

FIG. 9. The amplitude entropy variation comparison of wave fields built from Blackfoot 1227

Footprint of Bin Size

As a supplement of the analysis above, figure 10 explains why strong attenuation leads to small entropy values in our experiment. Subfigures in the left column imitate the possible amplitude distribution of a VSP snapshot. Suppose attenuation reduces the original amplitude by its 9/10 (from Figure 10-a to 10-b) while the bin size stays fixed as 1, there will be an observable change in the corresponding PDF. For data points are compressed in small values, many of them would fall into identical bins to form a relatively steep, concentrated PDF histogram. Further, will result in a small entropy value. Although attenuation would not have such strong effects in practice, the theory retains its rationality.

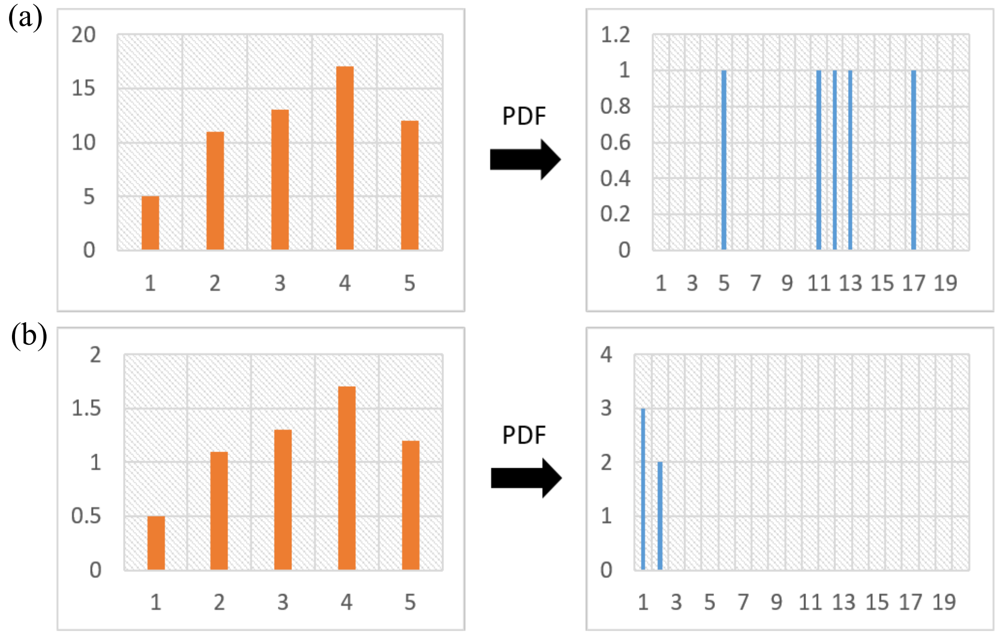

FIG. 10. Imitation of amplitude distribution in a VSP snapshot before and after attenuated and their corresponding PDF

Realizing bin size scale is the one of the key determinants of the entropy behaviour, we conducted another experiment to see how different bin sizes affect the entropy measurement in varying attenuating circumstance and more importantly, if the effect is strong enough to overthrow the opposite entropy reaction to intrinsic and extrinsic Q that we have observed. This new experiment contains two tests, the first one helps to track the footprint of the bin size scale and second one assesses the effect of unfixed bin size.

In the first test, we successively set bin size as 0.0001, 0.001 and 0.01. Figure 11 presents the entropy measurement of the wave fields in Figure 7-b (blue) and 7-c (red) under corresponding bin size. The bin size's increasement makes spikier entropy curve and reduces its magnitude but does not alter the interrelation of two entropy curves. In another word, the counteractive effect of absorption and stratigraphic filtering on entropy still holds.

In the second test, an unfixed, self-calculated bin size is adopted. Instead of giving a number beforehand, we stipulate that there are always 30 bins for the complete amplitude range and let the bin size to be calculated regarding every specific data set. The result in Figure 12 who has consistent characteristics with Figure 9 proves that this information measurement is more stable than we thought. No matter big or small, stationary or flexible bin size we choose, the conclusion of this research stays trustworthy.

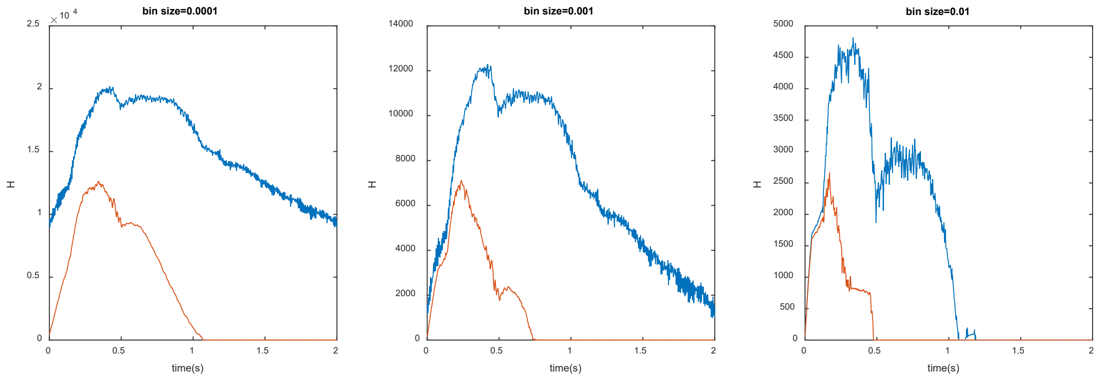

FIG. 11. Entropy measurements of wave fields in Figure 7-b (blue) and 7-c (red) under corresponding bin size

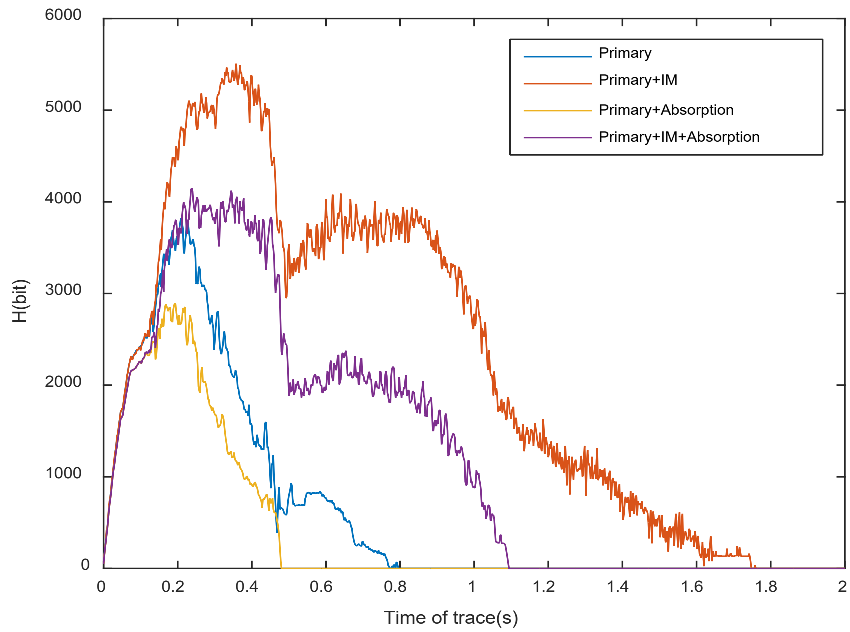

FIG. 12. Entropy measurements of Blackfoot 1227 using unfixed bin size

Frequency's impact on entropy

According to Spencer (1977), the attenuation in nonresolvable cyclic section vary with frequency in a different manner comparing to its linear dependence commonly attribute to absorption. This enlightened us to separate intrinsic and extrinsic Q from frequency analysis.

From this point of view, we infer that an entropy analysis of VSP wave field with varying frequency condition would somehow be informative. To manipulate the frequency condition in VSP, we provide the minimum phase wavelet with different dominant frequencies, then use them to construct the wave field. Calculate the entropy of the snapshots of these wave fields as before to get results in Figure 13. In here we are presenting outcomes with wavelet dominant frequency 65hz, 75hz and 85hz.

Figure 13-a represents the case when there is no apparent attenuation in wave field. Wave field ranges in higher frequency leads to a bigger entropy value because higher frequency sees more detailed subsurface structure and produces more reverberations.

In Figure13-b, internal multiples are added to the non-attenuating system. There are again higher pick entropies. Through this subfigure, the earlier statement seems to be true that internal multiples are only scattering waves in the wave field, because the entropy curves are displayed in the same order as in (a) but with bigger separation due to the involvement of internal waves.

Besides smaller peak entropies, curves in figure 13-c presents inverse relative position comparing to figure 13-a. This is due to the linear dependence of intrinsic Q attenuation upon frequency. The attenuation grows rapidly with ascending frequency so that it counteracted, even overwhelmed the original effects of ascending frequency on entropy. This is supported by the fact that intrinsic Q is usually stronger than extrinsic Q.

In this experiment, the impacts of internal multiples and absorption upon entropy are still counteracting each other. No further frequency analysis has been made due to the limited understanding of entropy, yet our confidence is strengthened to separate intrinsic and extrinsic Qs from this information measurement.

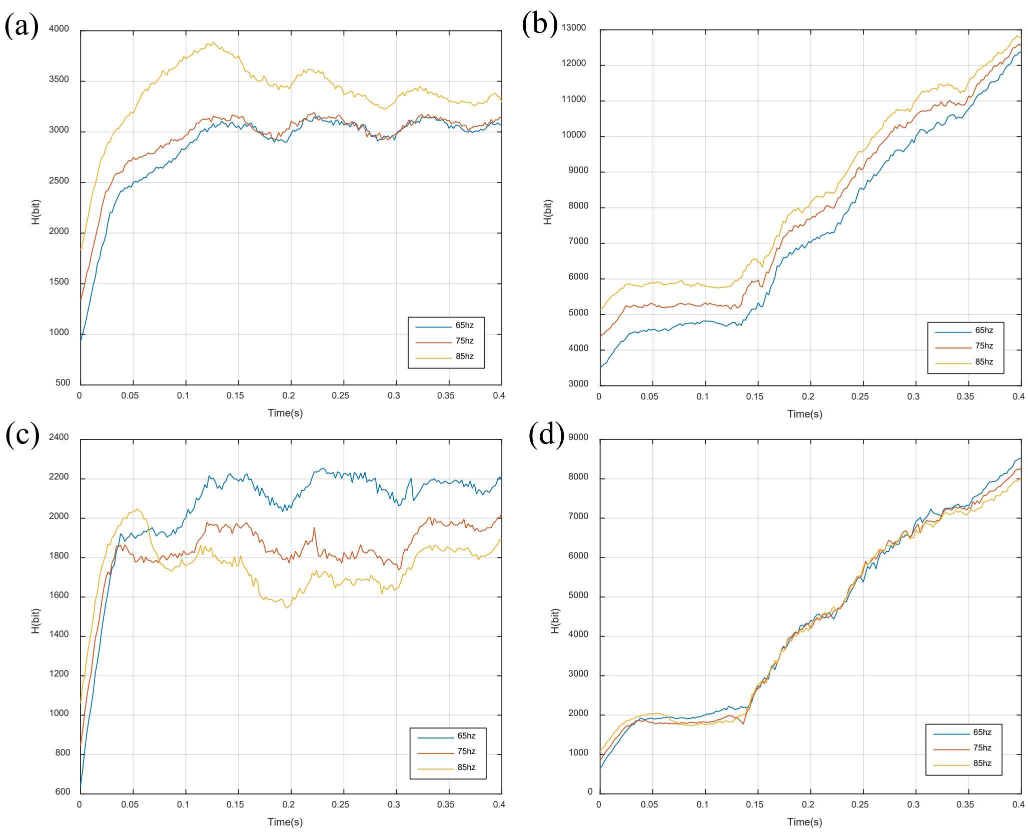

FIG. 13. Entropy measurements of wave fields with different dominant frequency wavelets: 65hz, 75hz and 85hz

CONDITIONAL SHANNON ENTROPY

The above analysis contains hints that a sensitive information or entropy based analysis could uncover differences between intrinsic and extrinsic attenuation. However, the statistics producing H are not sensitive to the correlations between nearby values of the wave field, and it seems likely that measures involving these correlations might do more to expose differences between extrinsic and intrinsic Q. Empirically we know that for a bandlimited seismic waveform, if at one position and time the displacement has a certain value, at a nearby position and the same time the displacement is not arbitrary, but is likely to lie nearby the first value. For example, in Figure 14, suppose the wave propagates to point A has amplitude 0.045. If we make prediction about point B, it is reasonable to say the chance amplitude at B falls between 0 and 0.05 will be bigger than the chance it be negative. In standard information theory, this is similar to the likelihood of finding the letter 'u' immediately after the letter 'q' in a selection from English text. Higher order information measures take account of these correlations in analyzing English; here we will investigate their usage in analyzing wave data.

An updated entropy calculation is then conducted on all well logs as follows. Only results from Blackfoot 1227 are illustrated in the following section for their results are quite similar. Besides adding practicality to the experiment, it is also foreseeable that the introduction of data points correlations will efficiently reduce the computation.

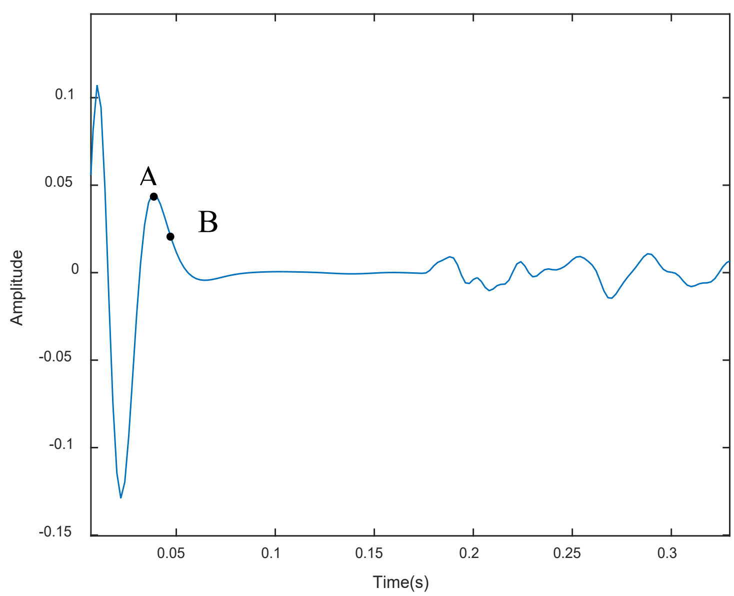

FIG. 14. A seismic wave example

The Conditional Algorithm

Instead of viewing data points independently, now take one amplitude value as prerequisite and compute the conditional probability distribution of amplitudes following it in the whole data set, the result is displayed in Figure 15. The probabilities distribute along diagonals, which means the subsequent correlates strongly with the preceding value.

In the new algorithm, if $H(Y|X=x_i)$ is the conditional entropy of variable Y with prerequisite X taking a certain value $x_i (i=1,2,\ldots n)$. And the PDF of X is $P(x_i)$, conditional PDF of Y is $P(y_j|x_i)$ (y_j represents every possible value of Y), then conditional entropy is defined as:

$$H(Y|X) = \sum_{x_i} P(x_i) H(Y|X=x_i) = -\sum_{x_i} P(x_i) \sum_{y_j} P(y_j|x_i) \log P(y_j|x_i) \qquad (8)$$

In our experiment, X is the prerequisite displacement U0, and Y stands for the adjacent (following) displacement Ui in Figure 15.

We calculate the new entropy of snapshots in wave field according to the work flow in Figure 16. The flow still uses statistical PDF for the first point in trace, and determines the entropy of it from equation (4). Then with conditional PDF of second point, the conditional entropy of second point can be computed from equation (8). In the next step, we update the PDF of second point with a new function P' which contains information of the first two points, and get entropy of third point from equation (8) again. Keep renewing PDF from the second to N-1th points, and add the entropies of N points up will give us the final result (Figure 17).

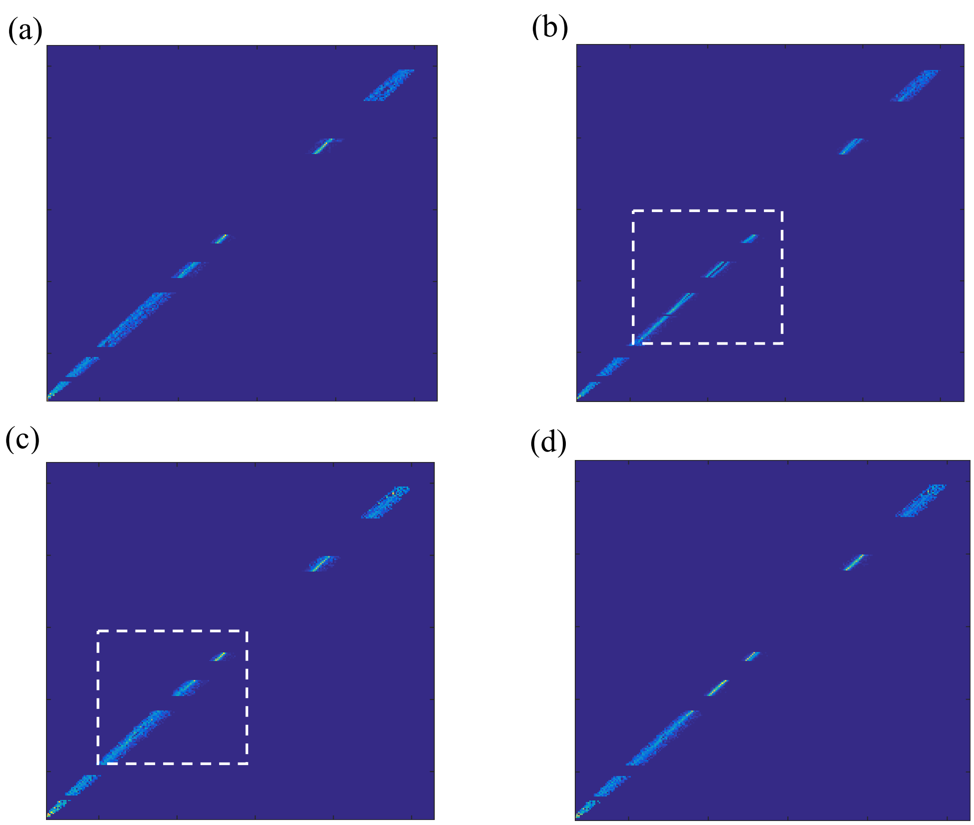

FIG. 15. Conditional PDF of amplitude Ui with prerequisite amplitude U0 from VSP data sets of Figure 3 (several points around zero amplitude are muted for their vastly big values against others). The white circles help focus on region with visible distinctions

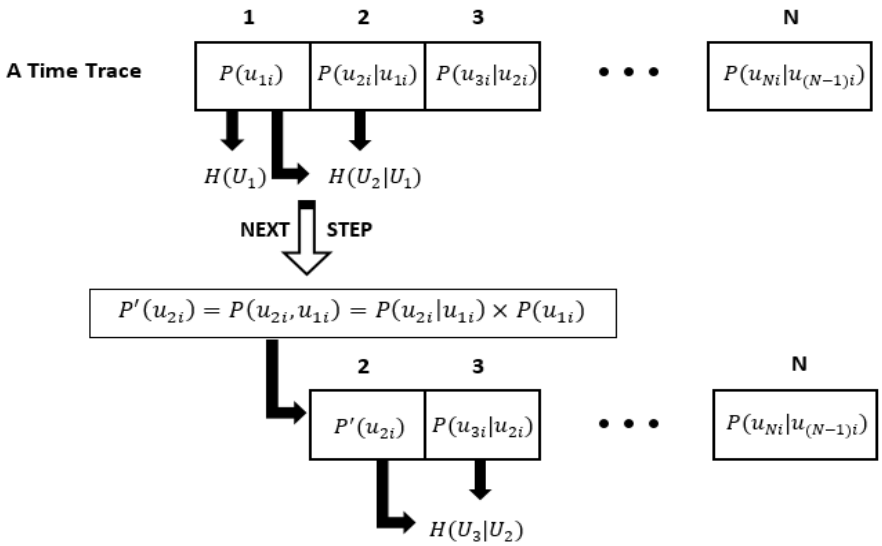

FIG. 16. Work flow of conditional entropy

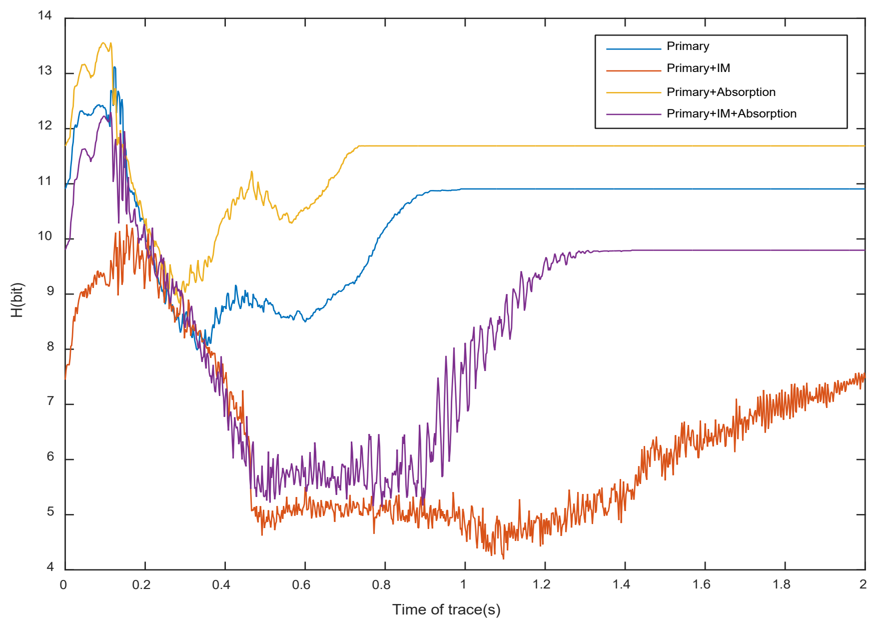

FIG. 17. The conditional amplitude entropy variation comparison of wave fields built from Blackfoot 1227

Figure 17 allows us to compare these new results to the originals in Figure 9—the zero-order entropy. The comparison leads to the following preliminary conclusions:

(1) The magnitude of the entropy values has been greatly reduced owing to the use of conditional probabilities meaning PDF histograms contain far fewer entries;

(2) Entropy peaks under effects of internal multiples (red and purple curves) are now smaller than those from system with no internal multiples (yellow and blue curves) , opposite to the results in Figure 9;

This seem unexpected at first, however, in the new algorithm, we are reducing the uncertainty of the amplitude values by making use of the natural extent of the waveform. Each wave represents a certain amplitude sequence so that more waves in field will make the subsequent points more determined, and then lead to a smaller entropy. Internal multiples, as an exterior factor, increase the complexity of wave field while absorption does the opposite by attenuating amplitudes and blending different events (i.e. primaries, internal multiples, etc.) together. This is proved by the tighter probability distribution in circled region of Figure 15-b than 15-c;

Seven well logs comparison

To sum up and generalize our research above, Figure 18 and 19 show comparisons of the zero-order entropy and conditional entropy measurements among all wells. Discrepancies exist among different well logs due to the diverse geological conditions around the well positions, nevertheless all curves hold the similar trend and interrelation as entropy measurements from Blackfoot 1227. This means our results are robust across at least three more or less randomly selected analysis areas.

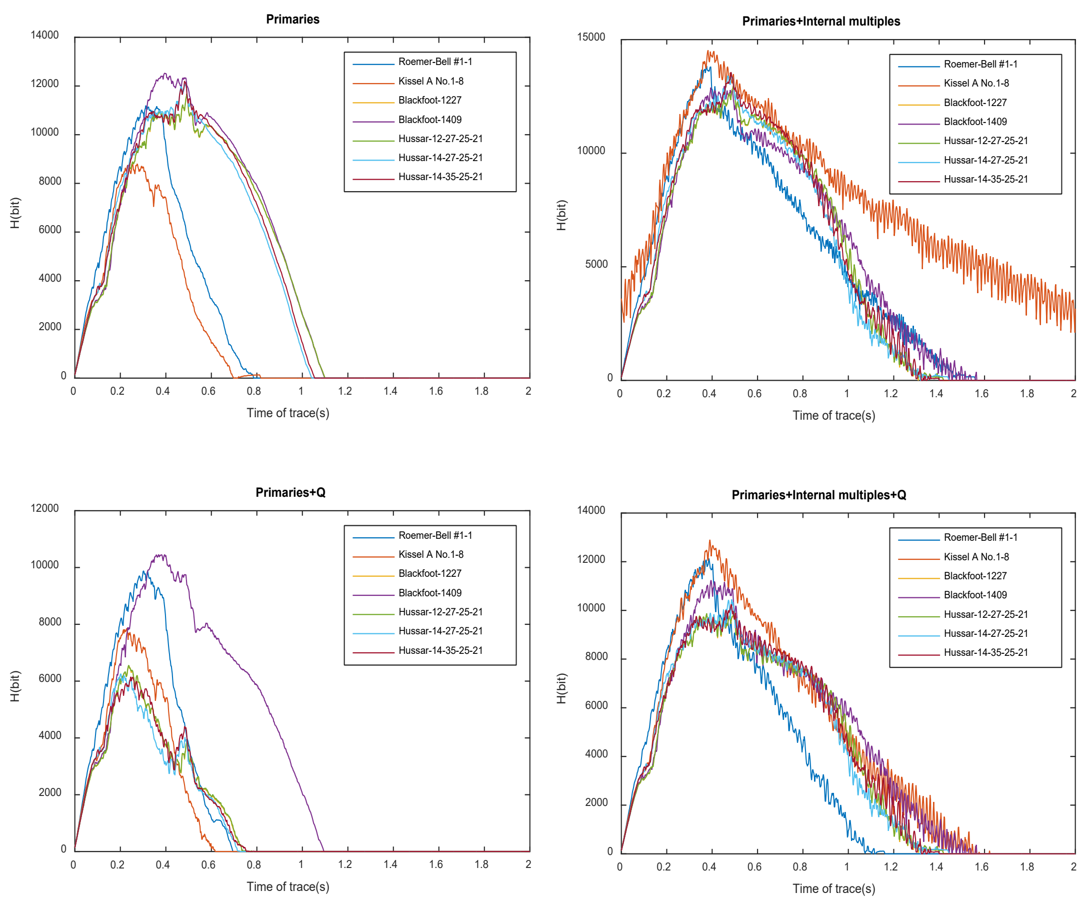

FIG. 18. Seven well log zero-order entropy comparison

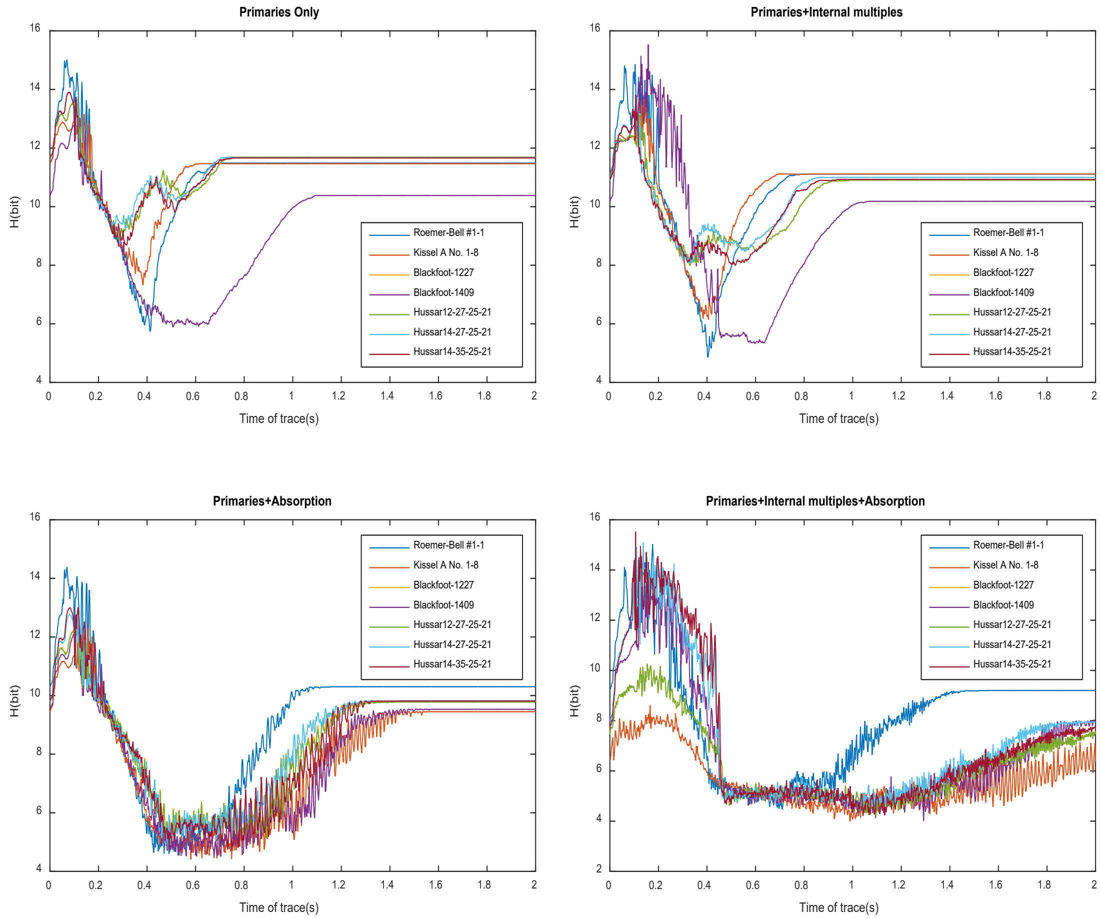

FIG. 19. Seven well log conditional entropy comparison

CONCLUSIONS

We are seeking measures of information that will help distinguish between intrinsic and extrinsic attenuation. This is important because rock physics based interpretation of Q values normally requires estimation of intrinsic Q, assuming extrinsic Q to be absent. Various entropy measurements appear to hold promise for this.

Although stratigraphic filtering and absorption produce very similar effects on propagating waves, from physical process point of view, they are different. Absorption transforms part of the wave energy into heats in an irreversible way while reverberations scatter energy to prevent them from completely transmitting through layers but leaving the overall energy intact. The advantage of Shannon entropy over some of the traditional methods that only deal with the attenuated transmitted waves is, it investigates into the wave field to monitor the functioning of the two mechanisms, serves as a magnifier that enhances these process differences, and translates them into a visible and measurable form.

Two entropy algorithms we used show very different results but analysis proves they are all reasonable. Although it cannot be decided yet if we should use the statistical entropy who has positive correlation with wave field complexity or conditional entropy who stays more rationality, reverberations and absorption always influence entropy variation in the opposite way in experiment, which is a promising start point to better evaluate the relative strength of stratigraphic dispersion and absorptive dispersion in a mixing effect scenario.

ACKNOWLEDGEMENTS

I want to thank my supervisor Dr. Kris Innanen for enlightening me with great ideas. Thanks to Dr. Gary Margrave and Wenyong Pan for helping me crack the code problem and CREWES sponsors for their financial support.

REFERENCES

Hauge, Paul S. "Measurements of attenuation from vertical seismic profiles." Geophysics 46.11 (1981): 1548-1558.

Innanen, Kris. "Blurring the line between intrinsic and scattering attenuation by means of the Shannon entropy." CREWES Research Report 24 (2012).

Lines, Larry, R. Phillip Bording, and Fereidoon Vasheghani. "Viscosity Estimation Using Seismic Inversion." CREWES Research Report 25 (2013).

Margrave, Gary F., S. Charles, and H. Aghabarati. "Intrinsic attenuation: removing the stratigraphic effect from attenuation measures." CREWES Research Report 27 (2015).

Margrave, Gary F. "Stratigraphic filtering and Q estimation." CREWES Research Report 26 (2014a).

Margrave, Gary F., and P.F. Daley. "VSP modelling in 1D with Q and buried source." CREWES Research Report 26 (2014b).

O'doherty, R. F., and N. A_ Anstey. "Reflections on amplitudes." Geophysical Prospecting 19.3 (1971): 430-458.

Resnick, J. R. "Stratigraphic filtering." pure and applied geophysics 132.1-2 (1990): 49-65.

Spencer, T. W., C. M. Edwards, and J. R. Sonnad. "Seismic wave attenuation in nonresolvable cyclic stratification." Geophysics 42.5 (1977): 939-949.

Spencer, T. W., J. R. Sonnad, and T. M. Butler. "Seismic Q-stratigraphy or dissipation." Geophysics 47.1 (1982): 16-24.

Stewart, Robert R., Phil D. Huddleston, and Tze Kong Kan. "Seismic versus sonic velocities: A vertical seismic profiling study." Geophysics 49.8 (1984): 1153-1168.

Vasheghani, Fereidoon, and Larry R. Lines. "Viscosity and Q in heavy-oil reservoir characterization." The Leading Edge 28.7 (2009): 856-860.

Walden, A. T., and J. W. J. Hosken. "An investigation of the spectral properties of primary reflection coefficients." Geophysical Prospecting 33.3 (1985): 400-435.